Electronic Supplementary Material (ESI) for Materials Advances.

ARTICLE

Preparation of noble metal-free porous CuO-ceria and zirconia mixed oxide catalysts by the ammonia driven deposition precipitation method for toluene combustion

Wouter Van Hoey [a], Anna Rokicińska [b], Marek Dębosz [b], Izabela Majewska [a], Piotr Kuśtrowski [b], Pegie Cool [a,*]

pegie.cool@uantwerpen.be

Supporting Information

S1: BJH Pore Size Distribution

Besides the determination of the specific BET surface area, the pore-size distribution can also be determined from N_2-sorption data. This can be done by using the Barrett, Joyner and Halenda (BJH) method, as described in the IUPAC technical report.[1] The BJH method is based on the assumption that condensation in the different pores will only occur if already several layers of gas adsorbed onto the walls of the pores. This assumption is made, because before the capillary condensation occurs, the pores are filled with gas by forming a monolayer and subsequently multilayers due to an increasing relative pressure. The resulting pore size distribution of the utilized $Ce_xZr_{1-x}O_2$ supports, obtained using the BJH method, is presented in **figure S1**. From this figure, it is clear that mesoporosity is introduced when cerium and zirconium are combined to generate a $Ce_xZr_{1-x}O_2$ mixed oxide support. When analyzing the pore size distribution of $Ce_{0.50}Zr_{0.50}O_2$, it is apparent that three different peaks can be identified around 3.7, 4.2 nm and 5.3 nm, respectively. This provides a first indication that a homogeneous ceria-zirconia mixed oxide with uniform pore sizes was not obtained for the corresponding material. Additionally, the same can be said about $Ce_{0.25}Zr_{0.75}O_2$, since besides a main peak around 3.7 nm, a broad shoulder is to be observed between 4 and 7 nm.

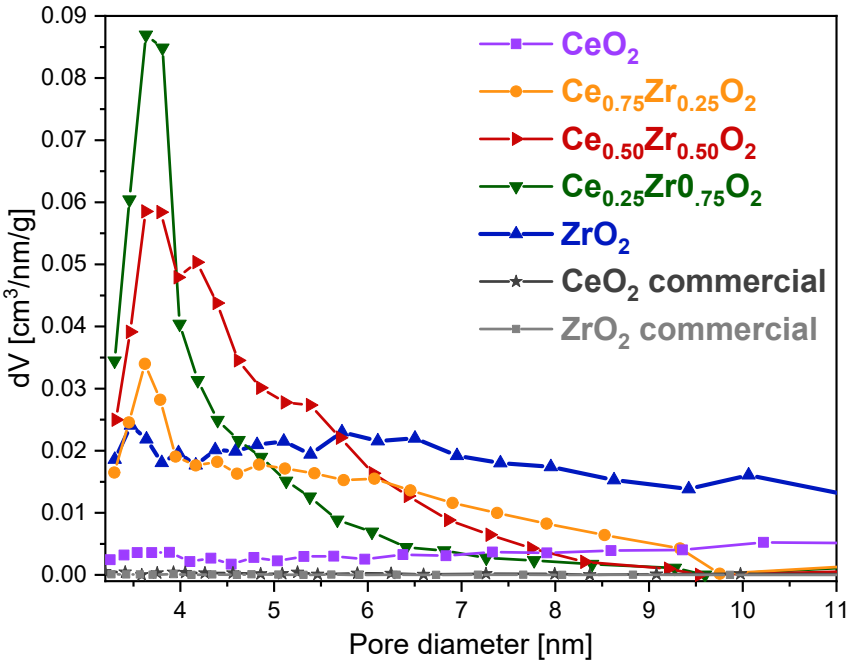

Figure S1: *BJH pore size distribution of the $Ce_xZr_{1-x}O_2$ support*

S2: Raman Spectroscopy

To support the information derived from the XRD patterns presented in part 3.1: Structural and textural properties of the $Ce_xZr_{1-x}O_2$ supports, Raman spectroscopy measurements were performed, which are presented in **figure S2**.

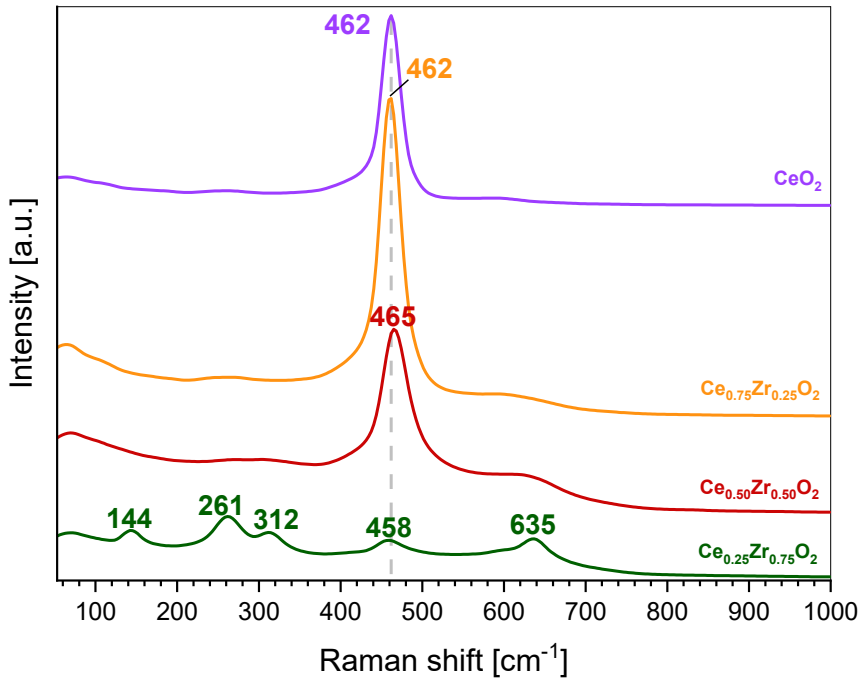

Figure S2: *Raman spectra of the $Ce_xZr_{1-x}O_2$ supports*

In the case of CeO_2, $Ce_{0.75}Zr_{0.25}O_2$ and $Ce_{0.50}Zr_{0.50}O_2$ one intense band centered around 462, 462 and 465 cm^{-1}, respectively, is observed. This band resembles the F_{2g} Raman mode of a cubic fluorite structure with space group Fm-3m, which is typically attributed to the symmetrical stretching vibration of a Ce-O_8 unit.[2] The strong intensity of the F2g band is caused by both the high symmetry of the ceria crystal structure and the polarizability of its Ce-O bonds.[2] When comparing the F2g band of pure ceria and $Ce_{0.50}Zr_{0.50}O_2$, a blue shift is noticed upon an increasing amount of zirconium. The reason thereof is the replacement of Ce^{4+} cations with smaller Zr^{4+} cations, which promote deformations of the CeO_2 crystal lattice. Additionally, as a result of the crystal lattice deformations, more defects are induced, generating more oxygen vacancies, resulting in a more pronounced shoulder between 560 and 680 cm^{-1}, which is associated to the longitudinal optical mode (LO) of CeO_2 that arises due to relaxation of symmetry rules.[3] For the $Ce_{0.25}Zr_{0.75}O_2$ support material, X-ray diffraction indicated that a cubic crystal structure was not retained and that a predominantly tetragonal crystal structure was formed. This is confirmed by Raman since the bands occuring at 144, 261, 312, 458 and 635 cm^{-1}, respectively, are characteristic for a tetragonal crystal structure with the P42/nmc space group.[2] Finally, apart from a tetragonal crystal structure, X-ray diffraction highlighted the presence of a monoclinic crystal phase for pure ZrO_2. Unfortunately, for ZrO_2, no Raman spectrum could be obtained. However, N_2-sorption data indicated that for ZrO_2 no uniform pore structure was obtained. Therefore, one could reason that for this material, the presence of the CTAB template had no significant impact on the porosity of the resulting material. Therefore, this material was re-synthesized in the absence of a template to investigate if a successful Raman spectrum could be recorded. After the synthesis of ZrO_2 with the same synthesis protocol but in the absence of a template, first an X-ray diffractogram was recorded. This way a direct comparison of the crystal structure of both ZrO_2 synthesized with and without CTAB could be made. The resulting comparison is presented in **figure S3** and indicates a strong similarity between both materials. In both diffractograms the reflections corresponding to the monoclinic (ICDD card: 00-013-0307) and tetragonal (ICDD card: 00-050-1089) phase structure of ZrO_2 are identified. However, it must be stated that in case of ZrO_2 synthesized in the absence of template, the reflection peaks corresponding to the monoclinic crystal phase are showing a stronger relative intensity in comparison to the tetragonal peaks than when CTAB is used during the synthesis. This suggests that the monoclinic crystal phase is slightly more present in the newly synthesized ZrO_2 without template.

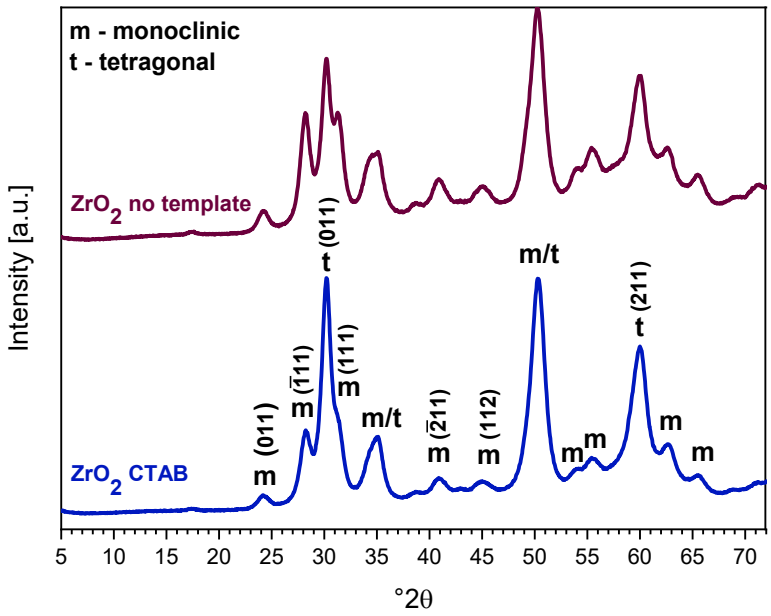

Figure S3: *XRD comparison of ZrO_2 synthesized with or without CTAB template*

After analyzing the XRD data presented in **figure S3**, it was attempted to record a Raman spectrum of the newly synthesized ZrO_2 in the absence of CTAB. This time a successful spectrum was recorded, which is presented in **figure S4** and proves the coexistence of monoclinic and tetragonal ZrO_2 crystal structure . As a result, because a clear Raman spectrum for ZrO_2 was succesfully obtained after alleviating the template during the synthesis, it is inferred that the presence of CTAB during the synthesis is responsible for the fact that no Raman spectrum could be obtained for ZrO_2. A possible explanation could be that the presence of CTAB affects the short-range interactions of neighbouring ions in the lattice.

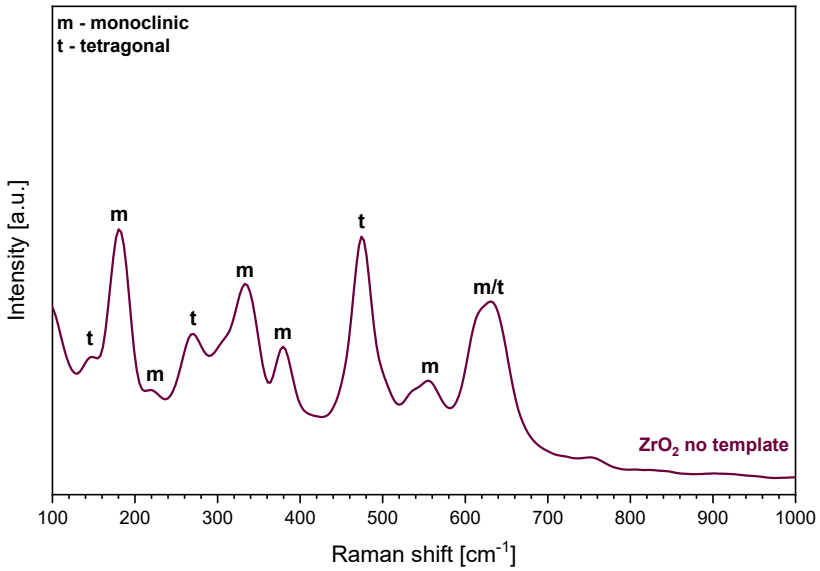

Figure S4: *Raman spectrum of ZrO_2 synthesized without CTAB template*

S3: Scanning Electron Microscopy (SEM)

Finally, SEM micrographs were recorded in order to offer an excellent visual examination of the structures formed during the synthesis of the $Ce_xZr_{1-x}O_2$ supports. The resulting images are presented in **figure S5**. First of all, the micrographs of zirconia show the formation of non-regular blocks where small aggregates can be seen on the surface. On the other hand, the surface of ceria looks totally different and exhibits a layer-like morphology. It is apparent that the formed layers are rather closely oriented and stacked. On top of that, needle-like particles are observable, which in accumulation resemble a cauliflower. In the case of the cerium and zirconium mixed oxides, a clear shape transition is visible. More specifically, $Ce_{0.25}Zr_{0.75}O_2$ maintains a similar profile as observed for ZrO_2, whereas $Ce_{0.75}Zr_{0.25}O_2$ exhibits characteristics pertaining to pure ceria, such as widely distributed needle-like particles on the surface. Furthermore, the micrograph of $Ce_{0.50}Zr_{0.50}O_2$ shows similarities with both $Ce_{0.25}Zr_{0.75}O_2$ and $Ce_{0.75}Zr_{0.25}O_2$.

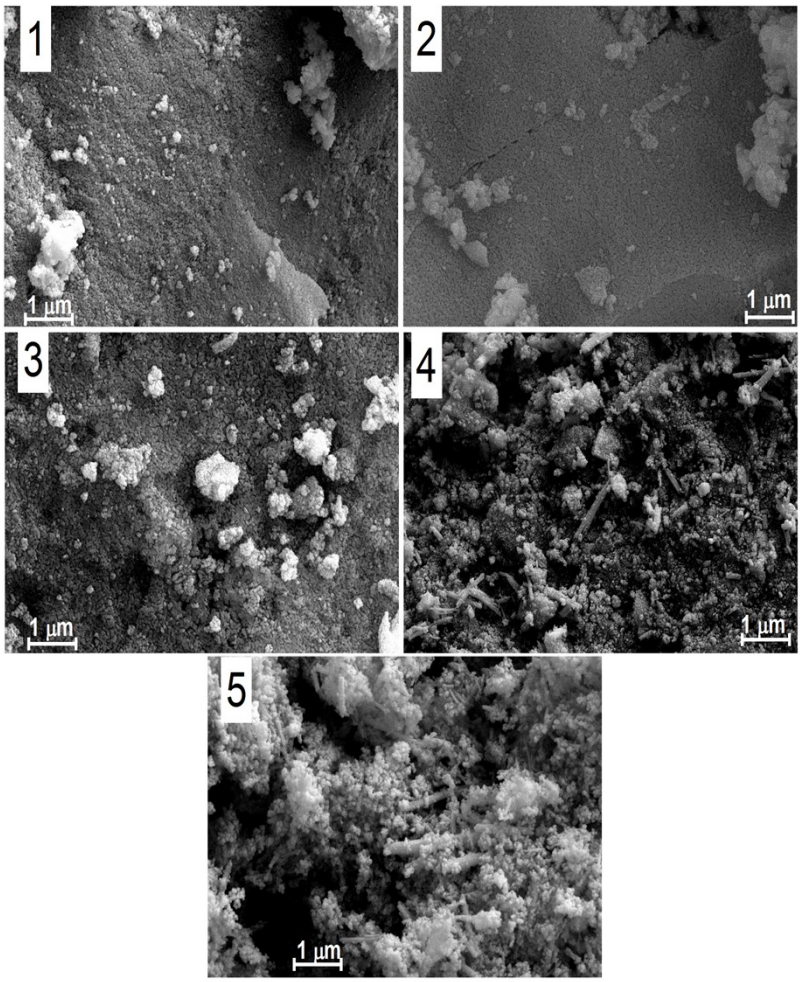

Figure S5: *SEM micrographs of (1) ZrO_2, (2) $Ce_{0.25}Zr_{0.75}O_2$, (3) $Ce_{0.50}Zr_{0.50}O_2$, (4) $Ce_{0.75}Zr_{0.25}O_2$ and (5) CeO_2*

S4: References

1 M. Thommes, K. Kaneko, A. V. Neimark, J. P. Olivier, F. Rodriguez-Reinoso, J. Rouquerol and K. S. W. Sing, *Pure Appl. Chem.*, 2015, **87**, 1051–1069.

2 S. Loridant, *Catal. Today*, 2021, **373**, 98–111.

3 R. C. R. Neto and M. Schmal, *Appl. Catal. A Gen.*, 2013, **450**, 131–142.